Advances in Geo-Energy Research

Vol. 2, No. 4, p. 369-379, 2018
www.astp-agr.com

Original article

A study of relative permeability for transient two-phase flow in a low permeability fractal porous medium

Zhenglan Li, Yonggang Duan*, Quantang Fang, Mingqiang Wei

State Key Laboratory of Oil and Gas Reservoir Geology and Exploitation, Southwest Petroleum University, Chengdu 610500, P. R. China

(Received July 6, 2018; revised July 25, 2018; accepted July 26, 2018; available online August 3, 2018)

Citation:
Li, Z., Duan, Y., Fang, Q., Wei, M. A study of relative permeability for transient two-phase flow in a low permeability fractal porous medium. *Advances in Geo-Energy Research*, 2018, 2(4): 369-379, doi: 10.26804/ager.2018.04.02.

Corresponding author:
*E-mail: nanchongdyg@163.com

Keywords:
Fractal theory
transient two-phase flow
relative permeability
threshold pressure gradient

Abstract:
In this paper, a relative permeability prediction method considering the effects of capillary pressure and threshold pressure gradient in a low permeability fractal porous medium is established and analyzed based on the fractal approximation model that porous medium consist of a bundle of tortuous capillaries. With this method, every parameter has clear physical meaning without empirical constants, and the model's predictions have a good agreement with experimental data. In addition to this, it makes some discussions that how the characteristic parameters (such as tortuosity fractal dimension, pore fractal dimension, ratio of minimum-maximum capillaries diameters and threshold pressure gradient) influence the relative permeability. This study may be conducible to a better understanding of the mechanism for transient two-phase flow in the low permeability fractal porous medium.

1. Introduction

It's a common phenomenon that experiments on low velocity flow in low permeability fractal porous media are not consistent with the classical Darcy's law. Thus threshold pressure gradient (TPG) is used to describe non-Darcy flow by some investigators (Thomas et al., 1968; Prada et al., 1999). In recent years, it has been shown that relative permeability plays an important role in the study of seepage flow mechanics for tight-sandstone porous medium (Hongen et al., 2012; Ofagbohunmi et al., 2012; Ding et al., 2014). Therefore, it's critical to find an analytical solution to obtain relative permeability considering the effects of threshold pressure gradient.

Because the microstructures of real porous medium are usually disordered and extremely complicated, at present, the relative permeability experiments and the numerical simulation calculation are the main methods to obtain the relative permeability curves. Many experiments have been carried out to obtain the relative permeability curves of low permeable sandstones (Mo et al., 2015; Zhang et al., 2017; Jeannin et al., 2018). Based on the experimental results of the low-permeability porous media, researchers proposed various empirical correlations including constants without physical meanings (Verma et al., 1984; Ge et al., 2014). Over the past 20 years, with the development of the parallel computing technology, Lattice Boltzmann Method (LBM) was employed to calculate the relative permeability in porous medium (Benzi et al., 1992; Xu et al., 2000). A pore-scale modeling approach is used to model the multi-phase flow and calculate gas/oil relative permeability curves (Laroche and Vizika, 2005). However, this method is computation-intensive and time-consuming. Novelly, some statistics methods based on artificial intelligence concept are introduced to determine water/oil relative permeability at various conditions (Ahmadi et al., 2016). Katz and Thompson (Katz et al., 1985; Krohn et al., 1986) used the scanning electron microscopy and optical data to propose that microstructures of porous media are fractal geometries whose pore-size distributions abide by the fractal scaling law. A gas-water relative permeability model in inorganic shale with nanoscale pores at laboratory condition and reservoir condition was proposed based on the fractal scaling theory (Zhang et al., 2018). Therefore, fractal theory was introduced into the research of seepage flow mechanics (Mandelbrot, 1982).

https://doi.org/10.26804/ager.2018.04.02.

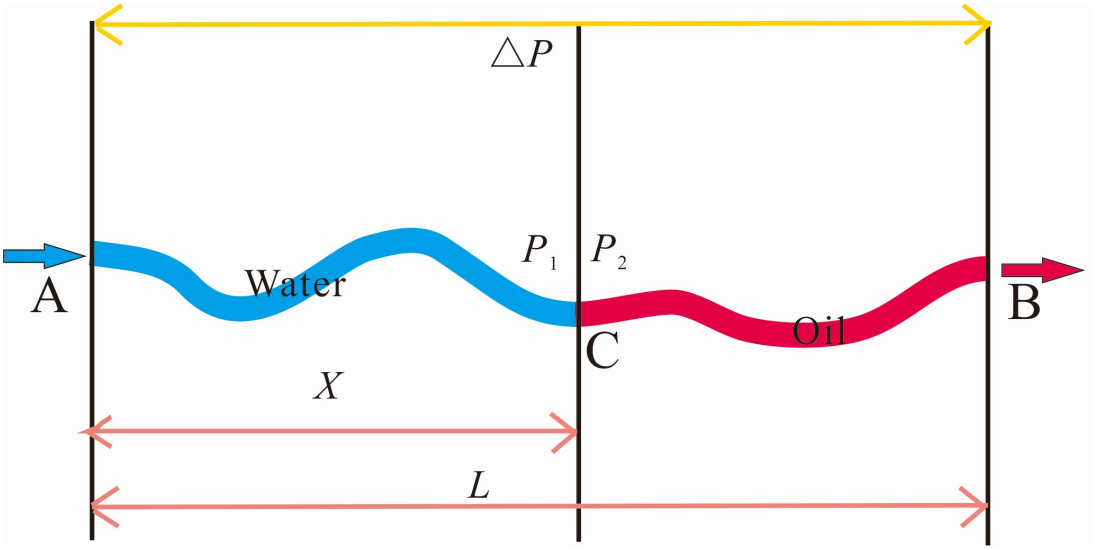

Fig. 1. Water-flooding flow in a single fractal capillary.

Delshad et al. (2003) established a pore-distribution model and deduced relative permeability and capillary pressure functions for two-phase flow. The simulation results agreed qualitatively with experimental data. Yu et al. (2004) derived analytical expressions for relative permeability based on models assuming that porous medium consist of a bundle of tortuous capillaries. However, this method didn't consider the effect of capillary pressure. Subsequently, Xu et al. (2013) took capillary pressure into account to predict the relative permeability of wetting phase. Based on the capillary bundle model and the fractal theory, a new nonlinear seepage equation was deduced, and a further fractal permeability model was obtained for oil transport in tight porous media by considering the effect of the boundary layer (Huang et al., 2017). Compared with Brooks-Corey models (Brooks et al., 1966), a good agreement was presented. Yun et al. (2008) obtained the analytical solution of threshold pressure gradient of Bingham fluid controlled by capillary pressure in fractal porous medium. Standnes presented a new model for estimating steady-state co- and counter-current relative permeabilities analytically derived from macroscopic momentum equations (Standnes et al., 2017). Cai (2014) analyzed the mechanism for fluid flow at low velocity and derived the expressions for velocity and flow rate of non-Newtonian fluid flow. Based on the collected experimental results, the Purcell's solution is modified and an improved solution considering the effect of boundary layer, Jamin and wettability is developed to determining the relative permeability curve (Tian et al., 2014). A novel predictive models for permeability and porosity of porous media considering stress sensitivity are developed based on the fractal theory and mechanics of materials by Tan et al. (2015). However, little research has been focused on relative permeability computation model in low permeability porous medium where threshold pressure gradient exists.

Relative permeability can be obtained by using the steady displacement or the dynamic displacement theory (water drive oil). Tan et al. (2014) derived a relative permeability model considering the effect of capillary pressure for transient two-phase flow, and analyzed the influence of fractal dimension on the shape of the relative permeability curve. Although the relative permeability curve has been obtained by him, there are some problems with this method. When it calculates the water saturation, it's based on the transient two-phase flow theory. While the relative permeability is obtained using the steady flow theory. Besides, Duan et al. (2015) and Lu et al. (2016) presented the relationship between water saturation and distance based on Buckley-Leverett solution and the impacts on water saturation were discussed. Whereas aforementioned fractal theory researches were all established on the basis of steady flow. So it's necessary to find the way to calculate the water saturation at the end face and oil or water relative permeability based on transient two-phase flow theory. Johnson et al. (1959) proposed the JBN method, a way to calculate relative permeability according to oil-water displacement experimental data. Therefore, in this paper, on the basis of above research, according to the fractal theory and water drive oil unsteady seepage theory, a modified JBN method is derived to calculate two-phase relative permeability, considering the effect of threshold pressure gradient and capillary force in the low permeability porous media.

2. Water-flooding flow in single fractal capillary

2.1 Single fractal capillary model

Before the study of the flow in the fractal porous media, an assumption was proposed that fractal porous media was made up of a bundle of tortuous capillaries with different diameters. At the beginning, the fractal capillary is only saturated with oil, later, the water is injected into the capillary and displaces the oil with a constant pressure difference (Δp) between point A and B. Ignoring the influence of the interphase mass transfer and phase change, there is an oil-water phase interface

in single fractal capillary at point C where pressures are unequal on both sides ($p_1 \neq p_2$) because of the influence of the capillary pressure (p_c). As shown in Fig. 1, oil (red) is displaced by water (blue) from point A to point B. L_T and L are the actual length and the straight distance of the fractal capillary respectively. X_T and X respectively stand for the actual length and the straight distance of the fractal capillary between point A and C ($0 \leqslant X \leqslant L$, $0 \leqslant X_T \leqslant L_T$).

2.2 Flow rate through single fractal capillary

The flow velocity through a single capillary is proposed by Hagen-Poiseuille (Bird et al., 2002). Based on Hagen-Poiseuille function, considering the effect of threshold pressure gradient, the water-phase flow velocity can be presented as follow:

$$v_w(\lambda) = \frac{\lambda^2(p_A - p_1)}{32\mu_w X_T} \cdot \left(1 - J_w \frac{X_T}{(p_A - p_1)}\right) \tag{1}$$

where J_w is the water-phase threshold pressure gradient; λ is the fractal capillary diameter; μ_w is the viscosity of water; p_A is the water-phase displacement pressure at the inlet A; and p_1 is the water-phase pressure at the interface C.

Similarly, flow velocity through a single capillary for oil can be expressed as:

$$v_o(\lambda) = \frac{\lambda^2(p_2 - p_B)}{32\mu_o(L_T - X_T)} \cdot \left(1 - J_o \frac{(L_T - X_T)}{(p_2 - p_B)}\right) \tag{2}$$

where J_o is the oil-phase threshold pressure gradient; μ_o is the viscosity of oil; and p_2 and p_B are the oil-phase pressure on the two-phase interface C and outlet B, respectively.

According to the theory proposed by Brown et al. (1951), the capillary pressure can be expressed as:

$$p_c = p_2 - p_1 = \frac{4\delta\cos\theta}{\lambda} \tag{3}$$

where δ is the surface tension; and θ is the contact angle.

The pressure difference between both ends of the core is:

$$\Delta p = p_A - p_B \tag{4}$$

Ignoring the compressibility of the fluid in th single fractal capillary, seepage velocities at anywhere in the capillary are equal to each other.

$$v_o = v_w \tag{5}$$

In Eqs. (1)-(5), parameters (v_o, p_1, p_2, p_A, p_B) are unknown. The flow velocity through a single capillary in a single fractal capillary is quantified by solving simultaneous Eqs. (1)-(5) above.

$$v(\lambda) = \frac{\lambda^2}{32} \cdot \frac{X_T(J_o - J_w) - L_T J_o + (\Delta p + p_c)}{(\mu_w - \mu_o)X_T + \mu_o L_T} \tag{6}$$

According to the fractal scaling law proposed by Wheatcraft and Tyler (1988), the actual length of the single fractal capillary (X_T, L_T) and the straight distance (X, L) have the following relationship:

$$L_T = L^{D_T} \lambda^{1-D_T} \tag{7}$$

$$X_T = X^{D_T} \lambda^{1-D_T} \tag{8}$$

where D_T is the tortuosity fractal dimension which characterizes the complexity of capillaries tortuosity in the porous medium. Substituting Eqs. (7) and (8) into Eq. (6):

$$v(\lambda) = \frac{\lambda^2}{32} \cdot \frac{\begin{pmatrix} \lambda^{D_T-1}\Delta p + 4\lambda^{D_T-2}\delta\cos\theta \\ -[X^{D_T}(J_w - J_o) + J_o L^{D_T}] \end{pmatrix}}{(\mu_w - \mu_o)X^{D_T} + \mu_o L^{D_T}} \tag{9}$$

Based on Eq. (9), multiply flow velocity by cross sectional area to get the transient two-phase flow rate.

$$q(\lambda) = \frac{\pi\lambda^2}{128} \cdot \frac{\begin{pmatrix} \lambda^{D_T-1}\Delta p + 4\lambda^{D_T-2}\delta\cos\theta \\ -[X^{D_T}(J_w - J_o) + J_o L^{D_T}] \end{pmatrix}}{(\mu_w - \mu_o)X^{D_T} + \mu_o L^{D_T}} \tag{10}$$

When $\delta = 0$ and $X = 0$ (or $X = L$) in Eq. (10), the equation of the transient two-phase flow rate is simplified into the one of single-phase flow rate.

$$q_s(\lambda) = \frac{\pi\lambda^2}{128} \cdot \frac{\lambda^{D_T-1}\Delta p - J_{o/w} L^{D_T}}{\mu_{o/w} L^{D_T}} \tag{11}$$

2.3 Oil-water interface position

Taking the derivative of the actual path length of water flow X_T with respect to the corresponding time t, the expression of the two-phase flow velocity can be expressed in another way.

$$v(\lambda) = \frac{\partial X_T}{\partial t} = \frac{\lambda^2}{32} \cdot \frac{\begin{pmatrix} \lambda^{D_T-1}\Delta p + 4\lambda^{D_T-2}\delta\cos\theta \\ -[X^{D_T}(J_w - J_o) + J_o L^{D_T}] \end{pmatrix}}{(\mu_w - \mu_o)X^{D_T} + \mu_o L^{D_T}} \tag{12}$$

Taking an integration of Eq. (12) with initial condition $t = 0$ and $X = 0$, there is a following relationship between the oil-water interface position X and corresponding time t.

$$\begin{aligned} 0 = {} & X^{2D_T} + \frac{2\mu_o L^{D_T}}{\mu_w - \mu_o} X^{D_T} \\ & - \frac{\lambda^{2D_T}\Delta p + 4\lambda^{2D_T-1}\delta\cos\theta - \lambda^{D_T+1} J_o L^{D_T}}{16(\mu_w - \mu_o)} t \end{aligned} \tag{13}$$

According to the Eq. (13), for a given certain moment t, a corresponding oil-water interface position X can be obtained. When $t = 0$, there is only oil saturating in the fractal capillary. As time goes on, the water is injected into the capillary and displaces oil until the breakthrough time t_D when the oil is completely displaced by water. The breakthrough time can be expressed as:

$$t_D = \frac{16(\mu_w + \mu_o)L^{2D_T}}{\lambda^{2D_T}\Delta p + 4\lambda^{2D_T-1}\delta\cos\theta - \lambda^{D_T+1} J_o L^{D_T}} \tag{14}$$

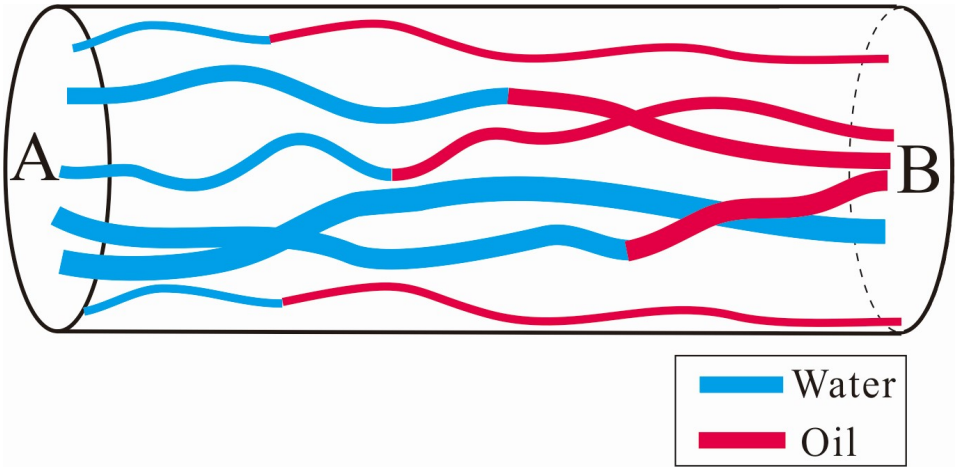

Fig. 2. Transient water-flooding flow in a porous medium at a certain time.

It is pointed out that breakthrough time is affected by the fluid properties and the capillary structure. Assuming other parameters (fractal dimension, viscosities of fluid, capillary length, pressure difference, threshold pressure gradient, contact angle and interfacial tension) are constant, the greater capillary diameter is, the less time need in the process of complete displacement.

3. Transient water-flooding flow in fractal porous media

3.1 Fractal porous media model

As is shown in Fig. 2, the relative permeability calculation method for transient two-phase flow in fractal porous media is based on the assumption that the fractal porous media is made up of a bundle of tortuous capillaries with different diameters. In a same capillary, the diameter is a constant at every point, but different capillaries have different diameters and vary continuously. The Eqs. (13) and (14) indicate that the capillaries with different diameters correspond to different interface positions for a given time, and the breakthrough times are different too. As for the capillaries with a bigger diameter, the flow velocity through a single capillary is faster than the smaller one so that the oil has been displaced by the water out of the cross-section B. On the contrary, these capillaries whose diameters are less than a certain threshold value are still saturated with two-phase fluid.

3.2 Critical capillary diameter

In order to calculate the oil and the water flow rate at the cross-section B respectively, it's necessary to distinguish the pattern of flow in every single capillary whether two-phase flow or not. Consequently, the critical capillary diameter λ_{cr} has been defined to judge whether the oil is displaced by water completely for a given time. Based on Eq. (14), the critical capillary diameter λ_{cr} can be obtained.

$$0 = \lambda_{cr}^{2D_T} + 4\lambda_{cr}^{2D_T-1}\frac{\delta\cos\theta}{\Delta p} - \frac{\lambda_{cr}^{D_T+1}J_oL^{D_T}}{\Delta p} - \frac{16(\mu_w+\mu_o)L^{2D_T}}{\Delta pt} \tag{15}$$

If $\lambda \geq \lambda_{cr}$, there is only single-phase flow in the capillary and the fluid out of cross-section B is water. On the contrary, if $\lambda < \lambda_{cr}$, the capillary is still saturated with two-phase fluid and the fluid out of cross-section B is oil. Therefore, the capillary should be divided into two parts to calculate the flow rate of oil and water.

3.3 Two-phase flow rate at the end face

In the case of two-phase fluid ($\lambda < \lambda_{cr}$), oil flow rate at the cross-section B can be derived by taking an integration of Eq. (10) from minimum pore diameter λ_{min} to critical capillary diameter λ_{cr}.

$$Q_o = -\int_{\lambda_{min}}^{\lambda_{cr}} qdN \tag{16}$$

According to the fractal geometry theory, the capillary diameters and the cumulative number of capillaries in fractal porous media obey the following fractal scaling law (Yu et al., 2002):

$$N(l \geq \lambda) = \left(\frac{\lambda_{max}}{\lambda}\right)^{D_f} \tag{17}$$

where N is the cumulative number of capillaries whose diameters are larger than λ; D_f is the pore fractal dimension; and λ_{max} is the maximum pore diameter. Take a derivative of Eq. (17) with respect to diameter λ, and then the number of capillaries within an infinitesimal range from λ to $\lambda + d\lambda$ can be expressed as:

$$-dN = D_f\lambda_{max}^{D_f}\lambda^{-(D_f+1)}d\lambda \tag{18}$$

Substituting Eq. (18) into Eq. (16), the expression of oil flow rate at the cross-section B can be obtained.

$$\begin{aligned} Q_o = & \frac{\pi D_f \lambda_{max}^{D_f} \Delta p}{128} \int_{\lambda_{min}}^{\lambda_{cr}} \frac{\lambda^{2+D_T-D_f}}{(\mu_w-\mu_o)X^{D_T}+\mu_o L^{D_T}} d\lambda \\ & + \frac{\pi D_f \lambda_{max}^{D_f} \delta \cos\theta}{32} \int_{\lambda_{min}}^{\lambda_{cr}} \frac{\lambda^{1+D_T-D_f}}{(\mu_w-\mu_o)X^{D_T}+\mu_o L^{D_T}} d\lambda \\ & - \frac{\pi D_f \lambda_{max}^{D_f}}{128} \int_{\lambda_{min}}^{\lambda_{cr}} \frac{(X^{D_T}(J_w-J_o)+J_o L^{D_T})\lambda^{3-D_f}}{(\mu_w-\mu_o)X^{D_T}+\mu_o L^{D_T}} d\lambda \end{aligned} \tag{19}$$

Similarly, in the case of single-phase fluid ($\lambda \geq \lambda_{cr}$), water flow rate at the cross-section B can be derived by taking a derivative of Eq. (11) from critical capillary diameter λ_{cr} to maximum pore diameter λ_{max}.

$$\begin{aligned} Q_w = & -\int_{\lambda_{cr}}^{\lambda_{max}} q dN \\ = & \frac{\pi D_f \lambda_{max}^{D_f} \Delta p}{128 \mu_w L^{D_T}(D_T+3-D_f)} (\lambda_{max}^{D_T+3-D_f} - \lambda_{cr}^{D_T+3-D_f}) \\ & - \frac{\pi D_f \lambda_{max}^{D_f} J_w}{128 \mu_w (4-D_f)} (\lambda_{max}^{4-D_f} - \lambda_{cr}^{4-D_f}) \end{aligned} \tag{20}$$

3.4 Average saturation in porous media

The total pore volume of porous media can be obtained by taking a derivative of the capillary volume from minimum pore diameter λ_{min} to maximum pore diameter λ_{max}.

$$\begin{aligned} V_P = & -\int_{\lambda_{min}}^{\lambda_{max}} \frac{\pi \lambda^2}{4} L_T dN \\ = & \frac{\pi D_f \lambda_{max}^{3-D_f} L^{D_f}}{4(3-D_T-D_f)} \left[1 - \left(\frac{\lambda_{min}}{\lambda_{max}}\right)^{3-D_T-D_f}\right] \end{aligned} \tag{21}$$

As is shown in Fig. 2, the pore volume occupied by water-phase is consist of two part: the whole volume of the capillaries whose diameters are greater than critical capillary diameter and the volume (blue part) occupied by water in capillaries whose diameters are less than critical capillary diameter.

$$V_w = -\int_{\lambda_{min}}^{\lambda_{cr}} \frac{\pi \lambda^2}{4} X_T dN - \int_{\lambda_{cr}}^{\lambda_{max}} \frac{\pi \lambda^2}{4} L_T dN \tag{22}$$

The volume of oil-phase in the porous media is only the red part of the capillaries whose flow regime is transient two-phase flow.

$$V_o = -\int_{\lambda_{min}}^{\lambda_{cr}} \frac{\pi \lambda^2}{4} (L_T - X_T) dN \tag{23}$$

Based on Eqs. (21)-(23), average water saturation and average oil saturation in porous media can be calculated with the following expressions respectively.

$$S_w = \frac{V_w}{V_P} = \frac{\frac{(3-D_T-D_f)}{L^{D_f}\lambda_{max}^{3-D_T-D_f}} \int_{\lambda_{min}}^{\lambda_{cr}} X^{D_T} \lambda^{2-D_T-D_f} d\lambda + \left[1 - \left(\frac{\lambda_{cr}}{\lambda_{max}}\right)^{3-D_T-D_f}\right]}{\left[1 - \left(\frac{\lambda_{min}}{\lambda_{max}}\right)^{3-D_T-D_f}\right]} \tag{24}$$

$$S_o = \frac{V_o}{V_P} = \frac{\frac{\lambda_{cr}^{3-D_T-D_f}}{\lambda_{max}^{3-D_T-D_f}} \left[1 - \left(\frac{\lambda_{min}}{\lambda_{cr}}\right)^{3-D_T-D_f}\right] - \frac{(3-D_T-D_f)}{L^{D_f}\lambda_{max}^{3-D_T-D_f}} \int_{\lambda_{min}}^{\lambda_{cr}} X^{D_T} \lambda^{2-D_T-D_f} d\lambda}{\left[1 - \left(\frac{\lambda_{min}}{\lambda_{max}}\right)^{3-D_T-D_f}\right]} \tag{25}$$

The average oil saturation and water saturation vary from 0 to 1. With the time t increasing, critical capillary diameter λ_{cr} decreases which makes the average oil saturation decline and the average water saturation rise.

4. Oil and water transition relative permeability

A method base on the fractal theory to calculate the oil-water relative permeability was derived by Tan et al. (2014). There are some problems with this method. When it calculates the water saturation, it's based on the transient two-phase flow theory. While the relative permeability is obtained using the steady flow theory. In addition to this, the water saturation at the end face should be used for drawing the relative permeability curve, not the average water saturation. So it's necessary to find the way to calculate the water saturation at the end face and oil or water relative permeability based on transient two-phase flow theory. In this part, a modified JBN method is derived to calculate relative permeability, considering the effect of threshold pressure gradient and capillary force in the low permeability porous media.

Based on the modification of Darcy's law for the threshold pressure gradient by Parad and Civan (1999), the non-Darcy seepage equations can be described as follows:

$$v_o = -\frac{k k_{ro}}{\mu_o} \left(\frac{\partial p_o}{\partial X} - J_o\right) \tag{26}$$

$$v_w = -\frac{k k_{rw}}{\mu_o} \left(\frac{\partial p_w}{\partial X} - J_w\right) \tag{27}$$

In Eqs. (26) and (27), k, k_{ro}, k_{rw} are the absolute permeability, oil relative permeability and water relative permeability in porous media, respectively.

Fluid fractional flow can be defined as the proportion of each kind of fluid flow rate in the total flow rate. Thus, the fractional flow of oil or water can be expressed as:

$$f_o = \frac{v_o}{v} \tag{28}$$

$$f_w = \frac{v_w}{v} \tag{29}$$

where v_o, v_w are oil-phase flow velocity and water-phase flow velocity, respectively; v is the sum of the two velocities above.

Substituting Eq. (29) into Eq. (27), the partial differential equation of water-phase pressure with respect to distance can be obtained.

$$\frac{\partial p_w}{\partial X} = -\frac{v f_w \mu_w}{k k_{rw}} + J_w \tag{30}$$

Take an integration of Eq. (30). Then the pressure difference can be obtained.

$$\Delta p = -\int_0^L \frac{\partial p_w}{\partial X} dX \tag{31}$$

According to Buckley-Leverett function. The moving velocity of the isosaturation surface in porous media can be expressed as:

$$\left.\frac{dX}{dt}\right|_{s_w} = \frac{q(t)}{\phi A}\frac{df_w}{dS_w} \tag{32}$$

where $q(t)$ is the water injection rate at time t. Take an integration of Eq. (32) from initial position X_0 to position X corresponding to time t, considering the initial condition ($X_0 = 0|_{t=0}$).

$$X = \frac{Q_{Iw}(t)}{\phi A}\frac{df_w}{dS_w} \tag{33}$$

When $X = L$, Eq. (33) should be changed into:

$$L = \frac{Q_{Iw}(t)}{\phi A} f'_{w_2} \tag{34}$$

Combining Eq. (33) and Eq. (34).

$$dX = \frac{L}{f'_{w_2}} df'_w \tag{35}$$

$$f'_{w_2} = \frac{1}{\overline{Q_{Iw}}} = \frac{AL\phi}{Q_{Iw}(t)} \tag{36}$$

where, f'_w is the derivative of the fractional flow with respect to water saturation; f'_{w_2} is the derivative of the fractional flow at the end face; $\overline{Q_{Iw}}$ is the multiple of cumulative injection pore volume; $Q_{Iw}(t)$ is the cumulative water injection volume at time t; A is the cross sectional area. Substituting Eqs. (30) and (35) into Eq. (31), the pressure difference can be obtained.

$$\Delta p = -\int_0^{f'_{w_2}} \left[\frac{v f_w \mu_w}{k k_{rw}} - J_w\right] \frac{L}{f'_{w_2}} df'_w \tag{37}$$

According to the relationship between the derivative of the fractional flow and the multiple of cumulative injection pore volume in Eq. (36), the water relative permeability at the end face of the porous media can be expressed as:

$$k_{rw_2} = f_{w_2}\left\{\frac{d\left[\frac{1}{\overline{Q_{Iw}}}\right]}{d\left[\frac{k(\Delta p + J_w L)}{v\mu_w L\overline{Q_{Iw}}}\right]}\right\} \tag{38}$$

The fractional flow is quantified by solving simultaneous Eqs. (26)-(29).

$$f_w(t) = \frac{\frac{\mu_o}{k_{ro}} + \frac{k}{v}\left[\frac{\partial p_c}{\partial x} + (J_w - J_o)\right]}{\frac{\mu_w}{k_{rw}} + \frac{\mu_o}{k_{ro}}} \tag{39}$$

Substituting Eq. (38) into Eq. (39), the oil relative permeability can be expressed as:

$$k_{ro_2} = \frac{\mu_o(1 - f_{w_2})}{\frac{\mu_w f_{w_2}}{k_{rw_2}} - \frac{k}{v}\left[\frac{dp_c}{dS_w}\frac{\partial S_w}{\partial x} + (J_w - J_o)\right]} \tag{40}$$

Assuming that the capillary pressure is a constant, Eq. (40) can be simplified to:

$$k_{ro_2} = \frac{\mu_o(1 - f_{w_2})}{\frac{\mu_w f_{w_2}}{k_{rw_2}} - \frac{k(J_w - J_o)}{v}} \tag{41}$$

Based on the material balance method, Welge et al. (1952) proposed that the water saturation at the end face B could be calculated using the following expression:

$$S_{w_2} = S_w - \frac{Q_{Iw}(t)}{V_P}(1 - f_{w_2}) \tag{42}$$

Through the study of the third part in this paper, it's pointed out that, for a given time t, the fractional flow at the end face f_{w_2} and the multiple of cumulative injection pore volume $\overline{Q_{Iw}}$ can be obtained by calculating the oil-phase flow rate Q_o and water-phase flow rate Q_w. And then substit uting all the known parameters into Eqs. (38), (41) and (42), the relative permeability k_{rw_2}, k_{ro_2} and the water saturation at the end face S_{w_2} can be obtained. Because different moment corresponds to different water saturation at the cross-section B, by changing the time t, the relative permeability curve can be drawn.

With this method, every parameter has clear physical meaning without empirical constants. In addition to this, fractal dimensions used for calculation reflect microstructures of real porous medium. Consequently, compared with traditional method to get the relative permeability, it's conducible to characterize the mechanism for transient two-phase flow in the low permeability fractal porous medium.

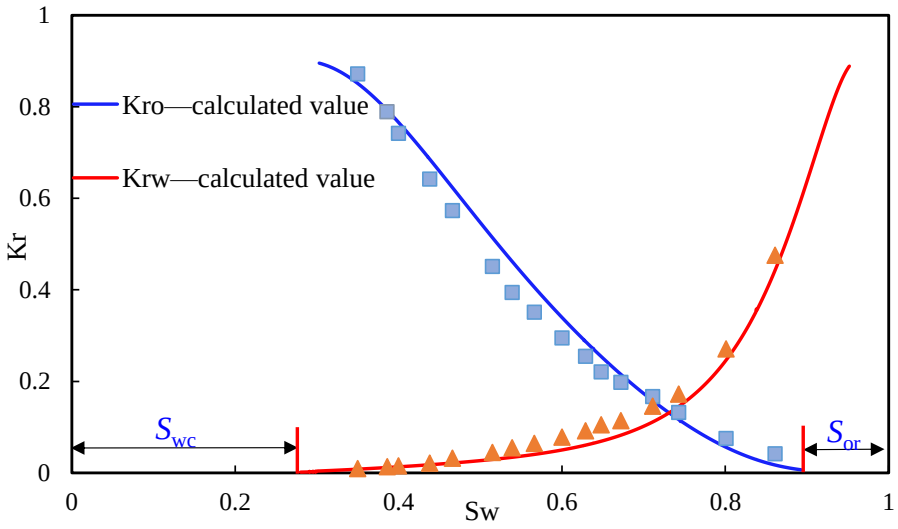

Fig. 3. Comparison of the actual relative permeability curve obtained by experiment with the theoretical prediction curve (L = 0.05 m, $\mu_w = 1\times10^{-3}$ Pa·s, $\mu_o = 5\times10^{-3}$ Pa·s, δ = 0.05 N/m, θ = 0.8, $J_o = 1.4\times10^4$ Pa/m, $J_w = 7\times10^3$ Pa/m, D_T = 1.1, D_f = 1.8, $\lambda_{min} = 4.3\times10^{-8}$ m, $\lambda_{max} = 2.6\times10^{-5}$ m, $\Delta p = 7\times10^5$ Pa).

5. Results and discussion

In order to verify the practicability of this method, the relative permeability calculation program was written to calculate the prediction values. Meanwhile, some experimental data in low-permeability porous media are provided by an oiler with water flooding improving recovery factor. The surface tension and the contact angle are obtained from the surface tension meter. The minimum and maximum capillaries diameters are measured by Micro-CT scanning and the constant-rate mercury injection experiments. Zhang and Liu (2003) supposed that the tortuosity fractal dimensions of the porous mediums are usually between 1.0 and 1.2. And the pore fractal dimension can be obtained according to the following expression (Yu et al., 2001):

$$D_f = d_E - \frac{\ln\phi}{\ln(\frac{\lambda_{min}}{\lambda_{max}})} \tag{43}$$

where d_E is Euclidean space dimension. In two dimensional Euclidean space, d_E = 2; while in three dimensional Euclidean space, d_E = 3. ϕ is the porosity of the porous medium. The theoretical relative permeability curve and experimental data into the same coordinate system are shown in Fig. 3. The models calculation results have a good agreement with the experimental data. This verifies the validity of the relative permeability prediction method for transient two-phase flow in low-permeability porous media.

It can be seen that the relative permeability of water-phase K_{rw} increases with an increase in water saturation S_w, but the relative permeability of oil-phase K_{ro} decreases instead. When the saturation approaches 1, the corresponding relative permeability also tends to 1. This result is matched with the actual physical phenomenon when water saturation turns to be irreducible water saturation ($S_w = S_{wc}$), the water relative permeability equals 0. Similarly, when oil saturation turns to be residual oil saturation (S_w = 1-S_{or}), the oil relative permeability decreases to 0. Additionally, the relationship $K_{ro} + k_{rw} < 1$ is also consistent with the fact.

Figs. 4 and 5 show the influence of the tortuosity fractal dimension D_T and the pore fractal dimension D_f on relative permeability curves, respectively. D_T describes the complexity of capillary tortuosity in porous media. The greater D_T is, the longer flow path of the fluid is. This may result in the decreasing of flow capacity. As is shown in Fig. 4, with the increase of D_T, oil relative permeability and water relative permeability both decrease. Similarly, the pore fractal dimension D_f represents the number and uniformity of pores in porous media. The number of capillaries with different diameters increases with an increase of D_f. Additionally, the heterogeneity of porous medium increases and the microstructure of pore becomes more complex. As is shown in Fig. 5, for a same given water saturation, both of the water and oil relative permeability decrease and the curves move down slightly with the increase of D_f.

Fig. 6 analyzes the influence of ratio of minimum-maximum capillaries diameters $\lambda_{min}/\lambda_{max}$ on relative permeability curves. It has the trend that the heterogeneity of porous medium increases while the ratio decreases. When $\lambda_{min}/\lambda_{max}$ approaches 1, all of the capillaries have a same diameter. That's to say, the porous media tends to be homogeneous. In Fig. 6, S_{or1}, S_{or2}, S_{or3} are the residual oil saturations under the different $\lambda_{min}/\lambda_{max}$. With the decreasing of $\lambda_{min}/\lambda_{max}$, the heterogeneous degree of porous media enhances so that both of the oil and water relative permeability decreases and the residual oil saturation increases. It's accord with the fact that the recovery is low in strong heterogeneity reservoir.

Fig. 7 shows that the relative permeability curves change with the different threshold pressure gradient. The relative

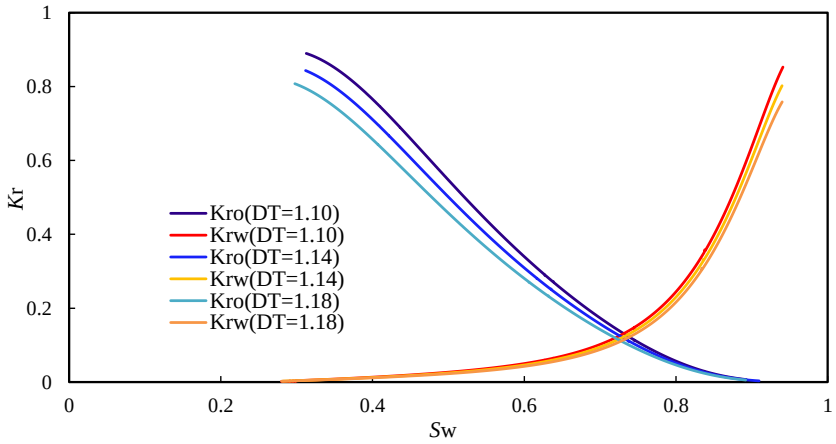

Fig. 4. The relative permeability curves affected by the tortuosity fractal dimension D_T (L = 0.05 m, μ_w = 1×10^{-3} Pa·s, μ_o = 5×10^{-3} Pa·s, δ = 0.05 N/m, θ = 0.5, J_o = 1.4×10^4 Pa/m, J_w = 7×10^3 Pa/m, D_f = 1.6, λ_{min} = 1×10^{-8} m, λ_{max} = 1×10^{-5} m, Δp = 7×10^5 Pa).

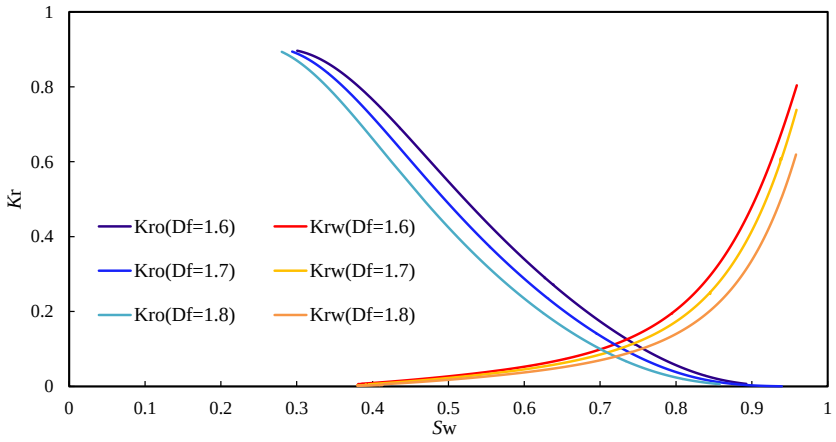

Fig. 5. The relative permeability curves affected by the pore fractal dimension D_f (L = 0.05 m, μ_w = 1×10^{-3} Pa·s, μ_o = 5×10^{-3} Pa·s, δ =0.05 N/m, θ = 0.5, J_o = 1.4×10^4 Pa/m, J_w = 7×10^3 Pa/m, D_T = 1.1, λ_{min} = 1×10^{-8} m, λ_{max} = 1×10^{-5} m, Δp = 7×10^5 Pa).

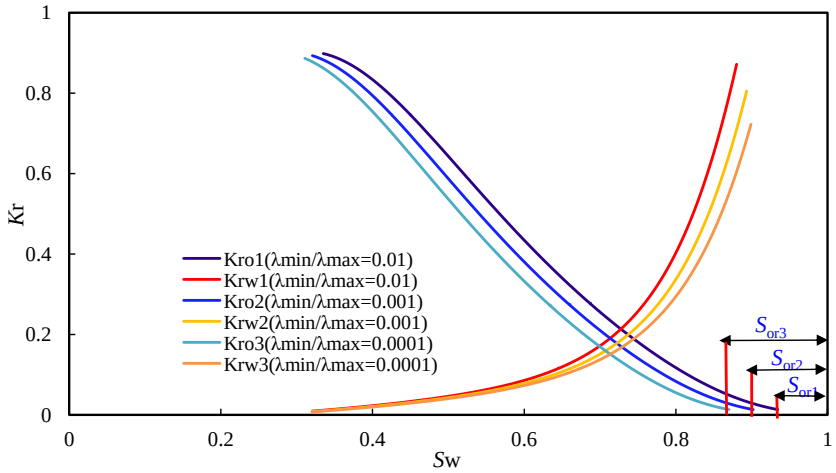

Fig. 6. The relative permeability curves affected by the ratio of minimum-maximum capillaries diameters $\lambda_{min}/\lambda_{max}$ (L = 0.05 m, μ_w = 1×10^{-3} Pa·s, μ_o = 5×10^{-3} Pa·s, δ = 0.05 N/m, θ = 0.5, J_o = 1.4×10^4 Pa/m, J_w = 7×10^3 Pa/m, D_f = 1.6, D_T = 1.1, Δp = 7×10^5 Pa).

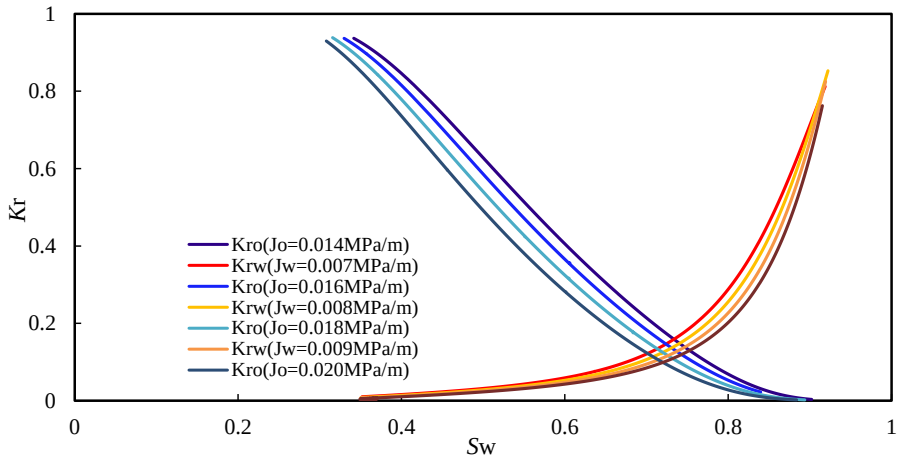

Fig. 7. The relative permeability curves affected by the threshold pressure gradient $J_{o/w}$ (L = 0.05 m, $\mu_w = 1\times10^{-3}$ Pa·s, $\mu_o = 5\times10^{-3}$ Pa·s, δ = 0.05 N/m, θ = 0.5, D_f = 1.6, D_T = 1.1, $\lambda_{min} = 1\times10^{-8}$ m, $\lambda_{max} = 1\times10^{-5}$ m, $\Delta p = 7\times10^5$ Pa).

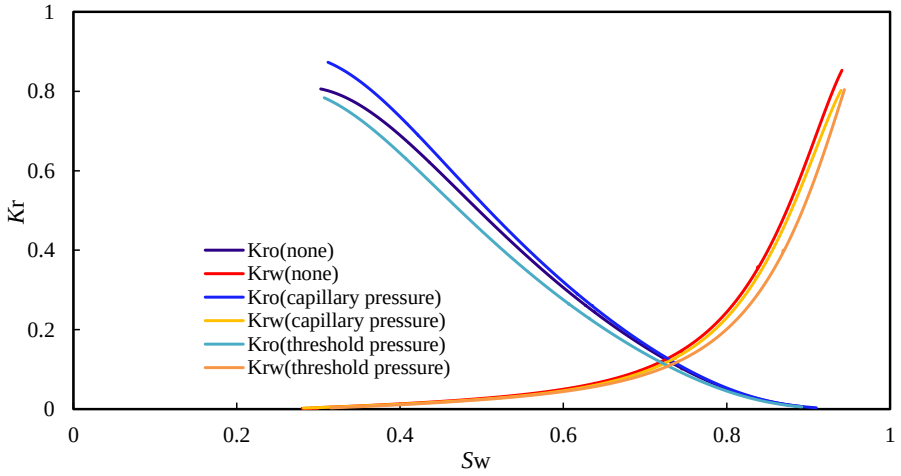

Fig. 8. The comparison of the influence of capillary pressure and threshold pressure on the relative permeability curves (L = 0.05 m, $\mu_w = 1\times10^{-3}$ Pa·s, $\mu_o = 5\times10^{-3}$ Pa·s, δ = 0.05 N/m, θ = 0.5, $J_o = 1.4\times10^4$ Pa/m, $J_w = 7\times10^3$ Pa/m, D_f = 1.6, D_T = 1.1, $\lambda_{min} = 1\times10^{-8}$ m, $\lambda_{max} = 1\times10^{-5}$ m, $\Delta p = 7\times10^5$ Pa).

permeability curves move down slightly with the increase of threshold pressure gradient. Because the oil-phase threshold pressure gradient is greater than water-phase threshold pressure gradient, generally, the oil-phase relative permeability curves decline more obviously.

Fig. 8 shows the relative permeability curves under three conditions. In the first case, there is neither the capillary pressure nor threshold pressure gradient, Considering the influence of the capillary pressure, the oil-water relative permeability was drawn in the same coordinate system with the first case. As for water-wet porous media, the capillary pressure is the driving force so that the oil-phase relative permeability curve rises. However, according to the Eq. (38), the water-phase relative permeability curve is almost unchanged. In the last case, considering the influence of the threshold pressure gradient, both the oil and water relative permeability curves move down. It's the difference between the general porous media and the low-permeability porous media. This result may be conducible to a better understanding of the mechanism for transient two-phase flow in the low permeability fractal porous medium.

6. Conclusions

We derived a relative permeability calculation method with the fractal theory, based on the fractal approximation model that porous medium consist of a bundle of tortuous capillaries. Different from the former research, the effects of threshold pressure gradient and capillary pressure have been taken into account. Besides, both the saturation and relative permeability are calculated with the transient two-phase theory not steady flow theory. With this method, every parameter has clear physical meaning without empirical constants. According to the sensitivity analysis of characteristic parameters (such as tortuosity fractal dimension, pore fractal dimension, ratio of minimum-maximum capillaries diameters and threshold pressure gradient), some conclusions have been obtained as

follows:

1) With the increase of fractal dimensions D_T and D_f, the structure of pore turns to be more complex. And it becomes harder to flow in fractal porous media which makes the relative permeability decrease.
2) For a given water saturation, it has a trend that the heterogeneity of porous medium increases if the ratio of minimum-maximum capillaries diameters $\lambda_{min}/\lambda_{max}$ decreases. As a result, the relative permeability decreases and the residual oil saturation increases instead.
3) Considering the effect of threshold pressure gradient, both the oil and water relative permeability curves move down. It's the difference between the general porous media and the low-permeability porous media. This result may be conducible to a better understanding of the mechanism for transient two-phase flow in the low permeability fractal porous medium.

Nomenclatures

D_T = Tortuosity fractal dimension
D_f = Pore fractal dimension
f' = Derivative of the fractional
f'_{w2} = Derivative of the fractional flow at the end face
J = Threshold pressure gradient
X_T = Actual path length
X = Straight distance
$Q_{Iw}(t)$ = Cumulative injection volume at time t
S = Saturation
d_E = Euclidean space dimension
k = Absolute permeability
k_r = Relative permeability
p = Water-phase displacement pressure
Δp = Pressure difference between A and B
$q(t)$ = Water injection rate at time t
t = Time
v = Flow velocity
ϕ = Porosity
λ = Fractal capillary diameter
λ_{cr} = Critical capillary diameter
μ = Viscosity
δ = Surface tension
θ = Contact angle

Subscripts

A = Inlet position A
B = Inlet position B
w = Water phase
o = Oil phase
min = Minimum value
max = Maximum value

Acknowledgments

This work was supported by the National Science and Technology Major Project of China (No. 2016ZX05015-003-04). The authors would like to appreciate reviewers and editors whose critical comments were very helpful in preparing this article.

References

Ahmadi, M.A., Zendehboudi, S., Dusseault, M.B., et al. Evolving simple-to-use method to determine water-oil relative permeability in petroleum reservoirs. Petroleum 2016, 2(1): 67-78.

Benzi, R., Succi, S., Vergassola, M. The lattice Boltzmann equation: Theory and applications. Phys. Rep. 1992, 222(3): 145-197.

Bird, R.B. Transport phenomena. Appl. Mech. Rev. 2002, 55(1): R1-R4.

Brooks, R.H., Corey, A.T. Properties of porous media affecting fluid flow. J. Irrig. Drain. Div. 1966, 92(2): 61-90.

Brown, H.W. Capillary pressure investigations. J. Pet. Technol. 1951, 3(3): 67-74.

Cai, J. A fractal approach to low velocity non-Darcy flow in a low permeability porous medium. Chin. Phys. B 2014, 23(4): 044701.

Delshad, M., Lenhard, R.J., Oostrom, M., et al. A mixed-wet hysteretic relative permeability and capillary pressure model for reservoir simulations. SPE Reserv. Eval. Eng. 2003, 6(5): 328-334.

Ding, Y.D., Wu, Y.S., Farah, N., et al. Numerical imulation of low permeability unconventional gas reservoirs. Paper SPE 167711 Presented at the SPE/EAGE European Unconventional Conference and Exhibition, Vienna, Austria, 25-27 February, 2014.

Dou, H., Yang, Y. Further understanding on fluid flow through multi-porous media in low-permeability reservoirs. Pet. Explor. Dev. 2012, 39(5): 674-682.

Duan, Y., Lu, T., Wei, M., et al. Buckley-Leverett analysis for transient two-phase flow in fractal porous medium. Comput. Model. Eng. Sci. 2015, 109-110(6): 481-504.

Ge, Y., Li, S., Qu, K. A novel empirical equation for relative permeability in low permeability reservoirs. Chin. J. Chem. Eng. 2014, 22(11-12): 1274-1278.

Huang, S., Yao, Y., Zhang, S., et al. A fractal model for oil transport in tight porous media. Transp. Porous Media 2017, 121(3): 725-739.

Jeannin, L., Bignonnet, F., Agostini, F., et al. Stress effects on the relative permeabilities of tight sandstones. C. R. Geosci. 2018, 350(3): 110-118.

Johnson, E.F., Bossler, D.P., Naumann, V.O. Calculation of relative permeability from Displacement Experiments. Trans. AIME 1959, 216: 370-372.

Katz, A.J., Thompson, A.H. Fractal sandstone pores: Implications for conductivity and pore formation. Phys. Rev. Lett. 1985, 54(12): 1325-1328.

Krohn, C.E., Thompson, A.H. Fractal sandstone pores: Automated measurements using scanning-electron-microscope images. Phys. Rev. B 1986, 33(9): 6366-6374.

Laroche, C., Vizika, O. Two-phase flow properties prediction from small-scale data using pore-network modeling. Transp. Porous Media 2005, 61(1): 77-91.

Lu, T., Duan, Y., Fang, Q., et al. Analysis of fractional flow for transient two-phase flow in fractal porous medium. Fractals 2016, 24(1): 1650013.

Mandelbrot, B.B. The fractal geometry of nature. New York, USA, WH Freeman, 1982.

Mo, S., He, S., Lei, G., et al. Effect of the drawdown pressure on the relative permeability in tight gas: A theoretical and experimental study. J. Nat. Gas Sci. Eng. 2015, 24: 264-271.

Ofagbohunmi, S., Chalaturnyk, R.J., Leung, J.Y.W. Coupling of Stress-Dependent relative permeability and reservoir simulation. Paper SPE 154083 Presented at the SPE Improved Oil Recovery Symposium, Tulsa, Oklahoma, USA, 14-18 April, 2012.

Prada, A., Civan, F. Modification of Darcy's law for the threshold pressure gradient. J. Pet. Sci. Eng. 1999, 22(4): 237-240.

Standnes, D.C., Evje, S,, Andersen P.Ø. A novel relative permeability model based on mixture theory approach accounting for solid-fluid and fluid-fluid interactions. Transp. Porous Media 2017, 119(3): 707-738.

Tan, X., Li, X., Liu, J., et al. Analysis of permeability for transient two-phase flow in fractal porous media. J. Appl. Phys. 2014, 115(11): 113502.

Tan, X., Li, X., Liu, J., et al. Study of the effects of stress sensitivity on the permeability and porosity of fractal porous media. Phys. Lett. A 2015, 379(39): 2458-2465.

Thomas, L.K., Katz, D.L., Tek, M.R. Threshold pressure phenomena in porous media. Soc. Petrol. Eng. J. 1968, 8(2): 174-184.

Tian, X., Cheng, L., Yan, Y., et al. An improved solution to estimate relative permeability in tight oil reservoirs. J. Pet. Explor. Prod. Technol. 2014, 5(3): 305-314.

Verma, A.K., Pruess, K., Tsang, C.F., et al. A study of two-phase concurrent flow of steam and water in an unconsolidated porous medium. Paper Presented at the 23rd ASME/AICHE National Heat Transfer Conference, Denver, 4-7 August, 1985.

Welge, H.J. A simplified method for computing oil recovery by gas or water drive. J. Pet. Technol. 1952, 4(4): 91-98.

Wheatcraft, S.W., Tyler, S.W. An explanation of scaledependent dispersivity in heterogeneous aquifers using concepts of fractal geometry. Water Resour. Res. 1988, 24(4): 566-578.

Xu, P., Qiu, S., Yu, B., et al. Prediction of relative permeability in unsaturated porous media with a fractal approach. Int. J. Heat Mass Transf. 2013, 64: 829-837.

Xu, Y., Wu, F. A new method for the analysis of relative permeability in porous media. Chin. Phys. Lett. 2002, 19(12): 1835-1837.

Yu, B., Cheng, P. A fractal permeability model for bi-dispersed porous media. Int. J. Heat Mass Transf. 2002, 45(14): 2983-2993.

Yu, B., Li, J. Some fractal characters of porous media. Fractals 2001, 9(3): 365-372.

Yu, B., Liu, W. Fractal analysis of permeabilities for porous media. Aiche J. 2004, 50(1): 46-57.

Yun, M., Yu, B., Cai, J. A fractal model for the starting pressure gradient for Bingham fluids in porous media. Int. J. Heat Mass Transf. 2008, 51(5-6): 1402-1408.

Zhang, B., Liu, X. Effects of fractal trajectory on gas diffusion in porous media. Aiche J. 2003, 49(12): 3037-3047.

Zhang, T., Li, X., Li, J., et al. A fractal model for gas-water relative permeability in inorganic shale with nanoscale pores. Transp. Porous Media 2018, 122(2): 305-331.

Zhang, Y., Osamu, N., Hyuck, P., et al. Relative permeability of CO_2 in a low-permeability rock: Implications for CO_2 flow behavior in reservoirs with tight interlayers. Energy Procedia 2017, 114: 4822-4831.